processes

MDPI

Article

Life Cycle Environmental Trade-Offs of Primary BOF Off-Gas Treatment

Jian Sun [1], Xiangang Tang [2], Dehai Bai [1], Hongjuan Bai [2], Dengfei An [2], Guangwen Zhou [2], Xiaohua Zhu [1,*], Mengxin Li [1], Yueming Gao [3] and Jian Yang [1,*]

[1] State Key Laboratory of Iron and Steel Industry Environmental Protection, Central Research Institute of Building and Construction Co., Ltd., MCC Group, Beijing 102629, China; sunjian7286@126.com (J.S.)
[2] Energy Saving and Environmental Protection Co., Ltd., Beijing 100088, China
[3] Beijing Key Laboratory of Resource-Oriented Treatment of Industrial Pollutants, University of Science and Technology Beijing, Beijing 100083, China
* Correspondence: zhu_xh2026@163.com (X.Z.); y_jian0812@163.com (J.Y.)

Abstract

Upgrading primary basic oxygen furnace (BOF) off-gas treatment changes pollutant removal, utility demand, and energy recovery simultaneously. Its life cycle benefits therefore depend on the energy actually displaced and the additional inputs required to recover it. We compare wet OG cleaning (S0), dry LT cleaning (S1), and sensible-heat recovery coupled with polyphenylene sulfide (PPS) filtration (S2), using treatment of the off-gas associated with 1 t of crude steel as the functional unit (FU). A complete BOF gas (BOFG) carbon balance separates eventual carbon oxidation from energy-substitution credits. The assessment retains an 18-category midpoint framework, while distinguishing the recalculated global warming potential (GWP) from screening-level non-climate estimates. Using the documented background proxies, central GWPs are 118.376, 108.622, and 102.304 kg CO_2-eq/FU for S0, S1, and S2 at 50% useful-heat utilization (S2-SS50), respectively. The 8.24% reduction from S0 to S1 is driven by lower utility demand and greater gas recovery. S2-SS50 achieves a further reduction of 5.82% relative to S1. Its heat-utilization break-even ratio is 0.86% under central assumptions, rises to 35.96% under an adverse operating combination with central energy factors, and reaches 82.64% when the energy background is also adverse. These deterministic scenarios show that the additional climate benefit of S2 depends on useful heat demand, operating inputs, and the displaced energy supply. Non-climate screening identifies possible burden shifts but does not establish an overall environmental ranking. Quantitative endpoint comparisons are withheld because they have not been recalculated consistently with the revised carbon inventory.

Keywords: life cycle assessment; basic oxygen furnace; primary off-gas; OG cleaning; LT cleaning; sensible-heat recovery; BOFG carbon balance

Check for updates

Academic Editor: Marco Ramírez-Argáez

Received: 26 September 2026
Revised: 15 October 2026
Accepted: 16 October 2026
Published: 22 October 2026

Copyright: © 2026 by the authors. Licensee MDPI, Basel, Switzerland. This article is an open access article distributed under the terms and conditions of the Creative Commons Attribution (CC BY) license.

1. Introduction

Decarbonizing steel production requires changes to the principal smelting routes, but it also depends on reducing energy losses and the burdens of pollution control within plants already in operation. Pang et al. [1] described the evolution of low-carbon steelmaking in China through improvements to the blast furnace–BOF route, exploration of alternatives to the blast furnace, and increasing integration of electricity and hydrogen into metallurgy. Kim et al. [2] compared the heat balances of ironmaking under air- and oxygen-based conditions, whereas Gao et al. [3] examined the carbon-reduction potential of coupling renewable

hydrogen production with a hydrogen-rich oxygen blast furnace. These studies concentrate on reduction chemistry and the main energy supply. For steelworks that continue to use the blast furnace–BOF route, off-gas cleaning and by-product energy recovery offer a distinct scope for retrofit. Primary BOF off-gas is hot, dust-laden, and rich in CO. Its treatment connects particle control with fuel recovery and sensible-heat management, requiring these functions to be assessed within a common environmental boundary.

In their review of air-pollution control in the steel industry, Yu et al. [4] examined source reduction, in-process control, and end-of-pipe treatment, linking pollutant formation to the technologies used for abatement. BOF dust formation and removal involve more than a change in total particulate mass. Li et al. [5] experimentally investigated the roles of bubble entrainment and elemental evaporation in dust generation. Li et al. [6] subsequently showed that agglomeration of zinc-bearing dust in a BOF gas-cleaning system is affected by Zn–Fe reactions and by constituents such as Na and K. A lower concentration of outlet dust thus describes only part of treatment performance. The composition of the captured solids, their subsequent recycling, and the energy consumed during gas cleaning also influence the environmental consequences of the process.

Dry cleaning changes both utility demand and the conditions under which captured dust can be recycled. Lanzerstorfer [7] studied air classification and in-plant recycling of electrostatic precipitator dust from converter steelmaking, calculating a 35–72% reduction in the mean number of zinc re-volatilization cycles. That study also discussed the engineering advantages of dry recovery and lower pressure drop. Combining experiments with analysis of an integrated steelworks, Andersson et al. [8] examined recycling routes for off-gas dust and emphasized the need to control zinc accumulation within the plant. The classification-based framework developed by Yang et al. [9] further identified the stability of $ZnFe_2O_4$ and the coupled presence of Cl and Pb as constraints on the selection of valorization routes. Together, these studies support coordinated design of dust removal and solids management. They do not, however, establish that each additional unit of captured dust displaces an equivalent amount of primary raw material.

Enhanced wet scrubbing and sensible-heat recovery provide different ways to improve primary off-gas treatment. Xu et al. [10] introduced waste-heat steam into a wet scrubber to promote condensational growth and capture of iron-rich particles approximately 200–300 nm in diameter. In their system, the outlet dust concentration fell from about 30–40 mg/m^3 to approximately 6 mg/m^3. Zhao et al. [11] conducted an industrial trial on a 100 t converter in parallel with an existing LT system. Replacing the evaporative cooler with a gas–solid separator and a waste-heat boiler increased steam generation and improved energy performance. The first of these studies demonstrates the potential to intensify wet particle removal; the second provides direct engineering evidence for reducing the sensible heat lost through evaporative cooling. In either case, the life cycle benefit must be evaluated alongside the additional operating and material inputs introduced by the modification.

The value of high-temperature off-gas also depends on energy quality and the conversion route. Chen et al. [12] used thermodynamic analysis to examine the feasibility of driving methane–CO_2 reforming with the residual heat of high-temperature BOF gas. Their work shows that chemical recovery is constrained jointly by off-gas conditions and the supply of reactants. In a review of electric arc furnace off-gas recovery, Yang et al. [13] distinguished sensible heat from chemical energy and examined their different uses. Although EAF and BOF gases arise under different operating conditions, these studies make an important distinction between heat recovered at the process, steam that can be delivered, and external energy that is actually displaced. Assessment of a sensible-heat recovery route must therefore account for heat demand and the timing of supply as well as the quantity of heat available.

Life cycle assessment (LCA) has revealed upstream burden shifting in advanced flue-gas treatment. Using 1 t of sinter as the functional unit, Cui et al. [14] evaluated an ultra-low-emission treatment chain and identified substantial contributions from wet denitrification and ozone oxidation, associated particularly with sodium sulfite, electricity, and liquid oxygen. In a comparison of three sintering flue-gas treatment technologies, Cui et al. [15] likewise found electricity to be an important environmental input across the routes, while the contribution of reagents varied with process configuration. Lower stack emissions therefore need not produce simultaneous improvements in every impact category. Sintering flue-gas desulfurization and denitrification nevertheless serve different functions from the cleaning of CO-rich BOF gas. Those studies cannot replace an explicit account of BOFG carbon oxidation and recovered-energy substitution when comparing primary BOF off-gas systems.

The use of steelworks by-product gases has expanded beyond direct heating to component separation and chemical synthesis. Uribe-Soto et al. [16] reviewed these thermochemical pathways. Lee et al. [17] performed a techno-economic analysis of methanol production from combined coke oven gas and BOFG, examining feed-gas proportions, process configuration, and heat integration. Bampaou et al. [18] investigated the integration of renewable hydrogen with steelworks gases for methanol and methane synthesis, showing that electrolysis can require more energy than is supplied by the feed gases themselves. These findings distinguish greater conversion or higher product value from lower environmental impact. Additional gas processing may create a useful product while also increasing energy demand, and its life cycle advantage cannot be inferred from the extent of resource recovery alone.

Environmental assessments of BOFG utilization demonstrate how the comparator and carbon destination change the result. de Kleijne et al. [19] compared heat supply, electricity generation, urea production, and scenarios involving carbon capture and storage, finding that displaced products and carbon fate can alter net climate impacts. Hense et al. [20] coupled process design with LCA for CO production from BOFG. Relative to conventional CO supply, the climate impact was about 10% lower with the German electricity mix and could be reduced by up to 68% under alternative scenarios involving renewable electricity and electrolytic hydrogen; mineral and metal resource consumption nevertheless increased. Eichwald et al. [21] integrated BOFG separation with phosgene production and identified differences in greenhouse-gas savings among separation processes and electricity backgrounds. These studies show why climate benefits and material-resource demand may diverge; both the additional processing inputs and the products displaced by recovery determine the environmental balance.

By-product energy use is also constrained by the internal energy network of a steelworks. In evaluating chemical uses of steel mill gases, Collis et al. [22] included the supplementary supply needed to replace their previous energy service, thereby accounting for the opportunity cost of diverting gas from an existing use. Qiu et al. [23] optimized a gas–steam–electricity network and demonstrated the coupling between the allocation of these energy flows. A related process-level perspective emerges from the comparative LCA of steel-slag treatment by Yang et al. [24]; the environmental differences among heat recovery, molten-slag modification, mineralization and cement co-processing depended on both treatment inputs and substitution benefits. Slag and off-gas differ in functional unit and carbon destination; thus, their impact values are not directly transferable. The shared methodological requirement is to separate the additional burden of treatment from the benefit of the recovered resource while maintaining an equivalent service basis.

Where a technology has not yet accumulated a long-term operating inventory, assessment must distinguish engineering potential from environmental performance under

specified conditions. Arvidsson et al. [25] recommended that prospective LCA state the technological maturity, scale-up assumptions, and background scenarios explicitly. Azimi and van der Spek [26] showed that electricity-background assumptions influence the comparison of prospective steelmaking routes. Previous BOFG studies have already assessed heat supply, power generation, and chemical production [19–22]. The question addressed here is more specific: how do wet OG cleaning, dry LT cleaning, and sensible-heat recovery with PPS filtration compare when they treat the same off-gas stream, retain the same eventual carbon-oxidation burden, and receive credits only for the energy services displaced?

Here, we compare those three routes using treatment of the primary off-gas associated with 1 t of crude steel as the functional unit. Wet OG cleaning is denoted as S0, dry LT cleaning as S1, and sensible-heat recovery with PPS filtration as S2. The contribution is the direct comparison of these treatment configurations under a common BOFG carbon balance and the explicit identification of the conditions governing the incremental climate benefit of S2. Operating inputs, BOFG recovery, and useful sensible-heat substitution are separated to identify the mechanisms behind each upgrade. An 18-category midpoint framework is retained, with non-climate estimates restricted to screening interpretation. Deterministic sensitivity and joint-scenario analyses then test how heat utilization, additional operating demand, and the energy background affect the climate break-even condition. This is not presented as the first LCA of BOFG utilization.

2. Materials and Methods

2.1. Process Routes and System Boundary

Three primary BOF off-gas treatment routes were evaluated. S0 represents conventional wet OG cleaning, comprising gas saturation and cooling, wet scrubbing, gas cooling, and treatment of the circulating water. S1 represents dry LT cleaning, comprising evaporative cooling, dry electrostatic precipitation, and BOFG recovery. S2 combines a dry cleaning route with low water demand, sensible-heat recovery, and PPS filtration. Five useful-heat utilization ratios were considered for S2: 0%, 25%, 50%, 75%, and 100%. The case in which 50% of recoverable heat is effectively used, denoted S2-SS50, provides the central scenario for comparison with S0 and S1.

The system boundary is defined for an incremental comparison of the off-gas treatment unit. It includes operating electricity and industrial water, PPS filter media and other quantified auxiliary inputs, direct emissions to air and water, BOFG recovery, and useful sensible heat delivered by S2. Ironmaking, the principal steelmaking operations, and processes identical across the three routes are not counted repeatedly in this incremental boundary. To close the carbon balance, however, eventual oxidation of the BOFG carbon associated with the functional unit is included in every route. Differences between routes are then expressed through upstream inputs, recovered gas, and useful-heat substitution. Equipment manufacture and infrastructure are excluded from the quantified baseline because a complete bill of materials was unavailable. Their omission limits the scope of the operating-stage comparison and the interpretation of the sensitivity results.

2.2. Functional Unit, Carbon Balance, and System Expansion

The functional unit (FU) is treatment of the primary BOF off-gas associated with production of 1 t of crude steel. All foreground inputs, direct emissions, recovered BOFG, and useful heat are expressed on this basis. Total BOFG generation is 100 Nm^3/FU in the central case. Unrecovered gas is 12 Nm^3/FU for S0 and 2 Nm^3/FU for both S1 and S2, giving recovered volumes of 88, 98, and 98 Nm^3/FU, respectively. For each route, indexed by s, the gas balance is $V_{gen} = V_{rec,s} + V_{loss,s}$. These central inputs define the compared operating

cases; the parameter ranges are examined separately rather than treating one operating point as representative of all steelworks. Net GWP is calculated as follows:

$$GWP_{net,s} = G_{BOFG,common} + GWP_{upstream,s} - C_{BOFG,s} - C_{heat,s}$$

In this expression, $G_{BOFG,common}$ is the eventual oxidation burden shared by all routes, calculated from total gas generation and the CO and CO_2 volume fractions. The BOFG substitution credit, $C_{BOFG,s}$, is determined from the volume actually recovered, a lower heating value of 8.5 MJ/Nm^3, a useful-energy efficiency of 0.85, and the GWP factor for displaced natural-gas heat. The term $C_{heat,s}$ is the credit for useful sensible heat from S2. With central CO and CO_2 fractions of 0.64 and 0.17, respectively, the common oxidation burden is 159.008 kg CO_2-eq/FU. Absolute results retain the complete carbon balance. Differences between routes, calculated after cancellation of the common carbon term, provide an independent consistency check. System expansion is applied to recovered BOFG and useful heat. Recovered solids receive no avoided-product credit because their quantity, composition, subsequent destination, and displaced product have not been established together.

The substituted product is defined by the energy service actually supplied in the model. Classifying a by-product gas as a recovered resource does not change the fossil origin of its carbon. Tenhumberg [27], in examining the accounting of fuels produced from steel mill gases, similarly showed that the energy source and accounting boundary influence the expression of greenhouse-gas savings. Useful heat supplied by natural gas is the explicit substitution reference here, and the resulting energy credit is calculated separately from the physical BOFG balance. Regulatory fuel classification is therefore not treated as evidence of physical carbon removal. This distinction ensures that recovered gas can receive a credit for displaced energy without its own eventual carbon oxidation disappearing from the inventory.

In the central carbon-balance scenario, recovered gas is subsequently combusted by an energy user, whereas the unrecovered fraction is assigned to flaring or non-recovery combustion without an energy credit. Thus, gas recovery changes the energy service delivered rather than removing fossil carbon from the system. With 100 Nm^3/FU of BOFG, CO and CO_2 volume fractions of 0.64 and 0.17, an ideal-gas molar volume of 22.414 Nm^3/kmol at 273.15 K and 101.325 kPa, and a CO_2 molar mass of 44 kg/kmol, eventual oxidation gives 159.008 kg CO_2/FU via every route. This is a modeled eventual-carbon-fate assumption, not evidence that all routes have identical stack CO concentrations or flare performance.

Natural-gas useful heat is the central substitution counterfactual, not an assertion that it is the marginal heat source at every operating hour. A transparent proxy is derived from the 2025 UK government conversion factors for natural gas (100% mineral blend): 0.20489 kg CO_2-eq/kWh for combustion and 0.03347 kg CO_2-eq/kWh for upstream well-to-tank supply, both on a net-calorific-value basis [28]. With an assumed useful-heat efficiency of 0.90, the factor is $(0.20489 + 0.03347)/(3.6 \times 0.90) = 0.073567901$ kg CO_2-eq/MJ of useful heat. The efficiency is a modeling assumption, with the 0.90 net-efficiency entry for industrial natural-gas heat production in the Ecoinvent 3.10 Change Report providing a reference point [29,30]. It is not a measured efficiency in the context of the studied enterprise. The UK supply factor is a geographical proxy, not a Chinese supplier-specific dataset. BOFG and additional sensible heat receive separate credits using this same factor. A scenario range of 0.0500–0.1000 kg CO_2-eq/MJ tests alternative displaced heat supplies; it is not a confidence interval for the UK natural-gas factor. Zero sensible-heat credit represents curtailment or no external heat displacement.

2.3. Life Cycle Inventory and Data Sources

The life cycle inventory was compiled from publicly available statistical yearbooks, published literature and information provided by a steelmaking enterprise. These source

types do not imply that every model input is a plant measurement. Table 1 identifies the central operating inputs, balance-derived quantities, and scenario assumptions; Table 2 reports the GWP factors used in the calculations. Following Arvidsson et al. [25], the technical and background conditions are stated explicitly. Supplementary Tables S1–S3 report the sensitivity bounds, heat-utilization scenarios, and joint boundary cases. Supplementary Table S4 records the source basis and the remaining documentation limits; Table S5 gives the central carbon balance, and Section S6 documents the background-factor derivation and additional checks. The numerical GWP calculations can therefore be reproduced from the tabulated inputs without relying on an unprovided workbook.

Table 1. Central inputs for the reproducible GWP comparison. All inputs refer to the FU of primary off-gas treatment associated with 1 t of crude steel. Fractions are dimensionless; a dash denotes an inapplicable input, not a missing measurement.

Parameter	Unit	S0	S1	S2-SS50	Basis
Electricity	kWh/FU	10.5	2.9	2.9	Technology-informed central cases; S2 net increment assumed zero
Industrial water	m^3/FU	0.40000	0.15000	0.12975	Central cases; S2 calculated from S1 minus 0.02025
PPS filter media	kg/FU	0.000	0.000	0.015	Aggregate engineering proxy
BOFG generated	Nm^3/FU	100	100	100	Literature-constrained common scenario
BOFG unrecovered	Nm^3/FU	12	2	2	Recovery-balance scenario
BOFG recovered	Nm^3/FU	88	98	98	Calculated as generation minus unrecovered gas
CO fraction	vol. fraction	0.64	0.64	0.64	Literature-informed composition assumption
CO_2 fraction	vol. fraction	0.17	0.17	0.17	Literature-informed composition assumption
BOFG lower heating value	MJ/Nm^3	8.5	8.5	8.5	Literature-informed central value
BOFG useful-energy efficiency	fraction	0.85	0.85	0.85	Engineering conversion assumption
Additional recovered steam	kg/FU	0	0	75	S2 engineering design case
Steam enthalpy increase	MJ/kg	—	—	2.33	Thermodynamic screening assumption
Useful-heat utilization	fraction	—	—	0.50	Central scenario; tested from 0 to 1
Recoverable sensible heat	MJ/FU	0	0	174.75	Calculated as 75 × 2.33
Useful sensible heat	MJ/FU	0	0	87.375	Calculated as 174.75 × 0.50

Electricity and industrial-water inputs were informed by technical information on dry BOFG recovery, while published studies constrained gas generation, composition, and lower heating value. The central inputs remain specified comparison cases rather than averages for all steelworks. For S2, 75 kg/FU of additional recovered steam and an enthalpy increase of 2.33 MJ/kg give 174.75 MJ/FU of recoverable sensible heat. At 50% useful-heat utilization, 87.375 MJ/FU displaces external heat. The steam term describes additional recovery represented for S2; it is not a claim that all other steam production in the steelworks is zero. The non-climate inventory also uses engineering estimates for dust characteristics, gaseous emissions, wastewater constituents, and material-related flows.

Those estimates do not constitute a complete, independently reproducible substance-level characterization inventory.

Table 2. Documented GWP factors and conversion constants. Values are used consistently across routes; unrounded derived values are retained in calculations.

Factor or Constant	Value	Unit	Basis and Scope
Electricity	0.5777	kg CO_2-eq/kWh	MEE 2024 national generation carbon-footprint factor, Table 1 [31]. Transmission/distribution additions are not included; Table 2 supplies gas/coal generation factors 0.4503/0.9240 for scenarios.
Industrial water proxy	0.1913	kg CO_2-eq/m^3	DESNZ 2025 full set, water supply, D18 [28]. UK mains-water supply proxy; not a plant-specific industrial-water or wastewater-treatment factor.
PPS material proxy	7.6	kg CO_2-eq/kg	Touré et al. [30], unfilled PPS average; reported range 6.9–8.6. Cradle-to-gate production/processing proxy; not a complete filter-bag lifecycle.
Displaced useful heat	0.073567901	kg CO_2-eq/MJ	Derived from DESNZ 2025 [28]: Fuels D45 + WTT- fuels D44, net CV, divided by 3.6 and assumed efficiency 0.90 [29]. UK fossil natural-gas supply proxy; see Section 2.2 and Supplementary S6.
Molar volume	22.414	Nm^3/kmol	Ideal-gas conversion at 273.15 K and 101.325 kPa (22.414 m^3/kmol); a physical conversion constant, not a lifecycle factor.
CO_2 molar mass	44	kg/kmol	Rounded stoichiometric molar mass; used consistently in all routes. Not an empirical background emission factor.

The central S2 electricity input is 2.9 kWh/FU, equal to S1. Zero additional electricity therefore means a net difference of zero between the complete S2 and S1 configurations; it does not mean that heat-recovery or filtration equipment consumes no power. This is a central engineering assumption, not a separately metered net saving. The additional electricity range of −0.67 to +5.0 kWh/FU tests the effect of possible savings or penalties, including pressure-drop and auxiliary-demand differences. The low central break-even threshold must be interpreted in conjunction with that assumption.

PPS filter-media consumption is represented by an aggregate input of 0.015 kg/FU, varied from 0.0045 to 0.0255 kg/FU. A plant-specific replacement inventory would divide the total mass of media replaced during a reporting period by the crude-steel throughput over that period. Equivalently, for steady operation, media demand is installed filter area multiplied by areal density, divided by service life and annual throughput. The present aggregate input does not separately establish filter area, areal density, or replacement interval. The PPS burden uses 7.6 kg CO_2-eq/kg, the average reported by Touré et al. [30] for unfilled PPS across the modeled processing technologies. Their cradle-to-gate study reported a range of 6.9–8.6 kg CO_2-eq/kg. This is a material-production proxy, not a filter-bag-specific cradle-to-grave dataset; it does not quantify textile fabrication, filter hardware, or end-of-life treatment.

2.4. Impact Assessment, Endpoint Indicators, and Normalization

The category framework follows ReCiPe 2016 (Hierarchist) [32] and retains the following 18 midpoint categories: global warming potential (GWP), stratospheric ozone depletion (SOD), ionizing radiation (IR), ozone formation affecting human health (OF-HH), fine particulate matter formation (FPMF), ozone formation affecting terrestrial ecosystems (OF-TE), terrestrial acidification (TA), freshwater eutrophication (FE), marine eutrophication (ME), terrestrial ecotoxicity (TET), freshwater ecotoxicity (FET), marine ecotoxicity (MET),

human carcinogenic toxicity (HCT), human non-carcinogenic toxicity (HNCT), land use (LU), mineral resource scarcity (MRS), fossil resource scarcity (FRS), and water consumption (WC). Freshwater eutrophication and freshwater ecotoxicity are distinct categories. The sums HCT+HNCT and TET+FET+MET shown in Figure 1 are diagnostic display groupings only; they are not additional, independently characterized ReCiPe categories and are not used for ranking. GWP is compiled from the documented CO_2-equivalent factors in Table 2 and the BOFG carbon balance, rather than obtained from a new substance-level ReCiPe characterization of every input. The source studies retain their own GWP characterization conventions; this compilation is not presented as a fully method-harmonized database calculation.

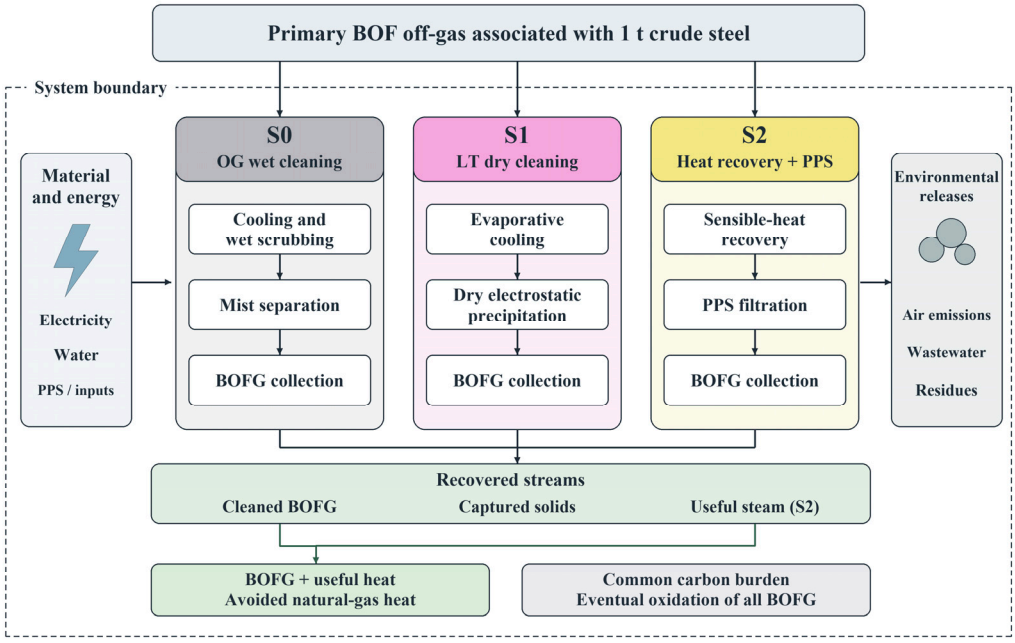


Figure 1. Process routes and life cycle system boundary for wet OG cleaning (S0), dry LT cleaning (S1), and sensible-heat recovery with PPS filtration (S2). In the central substitution scenario, recovered BOFG and useful sensible heat displace natural-gas heat. Eventual oxidation of the specified BOFG carbon remains within the boundary. No avoided-product credit is assigned to recovered solids in the GWP model. Boxes indicate process functions rather than detailed equipment designs.

Category-level normalization uses the ReCiPe 2016 v1.1 World 2010 H annual per-capita reference and expresses each category separately in person equivalents per functional unit (PE/FU). The GWP normalization factor is 7990.407653 kg CO_2-eq per person-year. No unweighted sum of the 18 normalized results is used. GWP is reconstructed from the complete BOFG carbon balance and the factors in Table 2. The other 17 plotted categories are inherited screening estimates rather than a new joint characterization of the revised inventory. Some contribution splits depend on equivalent-flow or recovered-solid proxies for which a mass-based substitution relationship is unavailable. These splits are not treated as measured emissions, validated avoided-product credits or quantitative causal attribution. Recovered-solid credits are excluded from the GWP model. Normalization does not resolve missing information with regard to the inventory or characterization.

For a reproducible non-climate characterization, each foreground flow must be linked to its quantity, physical unit, source, background dataset, and method version. Direct releases additionally require a substance identity and receiving compartment; particulate and metal releases require the relevant size and chemical speciation. Concentrations alone are insufficient without the corresponding gas or water volume. Equivalent units such

as kg Cu-eq and kg oil-eq are characterized proxies, not physical masses of metal wear or lubricant. Similarly, a dimensionless recovered-solid quality factor cannot define an avoided-product credit. Because that complete mapping was not available for the retained non-climate profiles, their interpretation remains exploratory.

2.5. Parameter Sensitivity and Useful-Heat Scenarios

One-factor-at-a-time deterministic sensitivity analysis was used to evaluate the GWP response of each route to key inputs. Each parameter was set to its low and high bound while all other inputs were held at their central values. Bounds were defined individually from the specified engineering range of each variable, rather than by applying a uniform percentage change. For S0 and S1, the analysis covers electricity, industrial water, BOFG loss, and shared energy parameters. For S2, it covers additional electricity and changes in water use relative to S1, recovered steam, useful-heat utilization, PPS input, and the shared energy parameters. Table S1 provides the input ranges and corresponding responses. The heat-factor bounds describe alternative substitution backgrounds, not variability around one measured supplier; Section S6 separately tests the published PPS-factor range. The radar charts report the percentage change from the central GWP of each route:

$$r_{s,p}^{L/H} = 100\% \times \frac{GWP_s\left(p^{L/H}\right) - GWP_{s,0}}{GWP_{s,0}}$$

where s identifies the route, p the varied parameter, L/H its low or high input, and $GWP_{s,0}$ the central result for that route. Because the widths of the parameter ranges differ, the response spans measure influence within the specified bounds. They are not normalized sensitivity coefficients for equal relative perturbations. A larger radial span can reflect both a stronger model response and a wider tested input range, and the radar polygon area is not used as a measure of route performance.

The incremental climate effect of S2 relative to S1 is evaluated as $\Delta GWP_{2-1} = GWP_2 - GWP_1$. Shared background factors are changed consistently in both routes. The central scenario applies the natural-gas useful-heat factor to both BOFG and sensible-heat substitution. Useful-heat utilization is evaluated at 0%, 25%, 50%, 75%, and 100%, followed by deterministic combinations of operating inputs and energy factors. A separate zero sensible-heat-credit case tests the absence of external heat displacement while leaving the common BOFG use unchanged. Neither parameter bounds nor joint combinations are probability distributions or confidence intervals. Non-GWP categories are outside the quantitative sensitivity analysis. Equipment manufacture is excluded from the baseline, but an analytical embodied-impact allowance is calculated to show how an additional net burden would affect the S2–S1 comparison.

3. Results and Discussion

3.1. Environmental Profiles Across the Three Routes

Figure 2 compares the relative profiles of the three routes across 18 midpoint categories. Results are expressed relative to the largest absolute value within each category, with the sign of the original result retained. The figure therefore shows differences among treatment routes within individual categories; bar heights across categories do not represent their relative environmental importance.

The GWP results in Figure 2 show a progressive reduction from wet OG cleaning to dry LT cleaning and subsequently to heat recovery with PPS filtration. The corresponding absolute impacts are 118.376, 108.622, and 102.304 kg CO_2-eq/FU for S0, S1, and S2-SS50, respectively. The transition from S0 to S1 reduces GWP by 9.754 kg CO_2-eq/FU, or 8.24%. This improvement reflects both the decrease in electricity consumption from 10.5 to 2.9 kWh/FU

and the increase in BOFG recovery from 88 to 98 Nm^3/FU. S2-SS50 provides a further reduction of 6.318 kg CO_2-eq/FU, or 5.82%, relative to S1, through the substitution of external heat by recovered sensible heat. Its cumulative reduction relative to S0 reaches 13.58%. These magnitudes depend on the background proxies and substitution conditions described in Table 2.

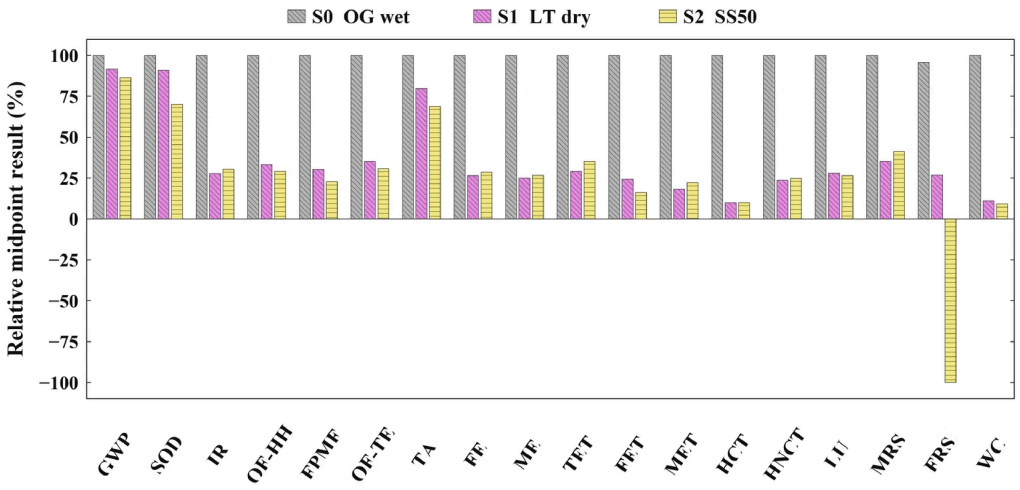


Figure 2. Relative profiles across 18 midpoint categories. Within each category, the largest absolute scenario value is set to 100%, retaining signs; this is not PE normalization. GWP is recalculated using the complete BOFG carbon balance and documented factors in Table 2.

These changes are consistent with the engineering mechanisms described in previous studies, although the configurations and assessment boundaries differ. Lanzerstorfer [7] examined the operational and solids-management characteristics of dry converter-gas cleaning, providing context for the reduced utility demand of S1. Xu et al. [10] demonstrated that intensified wet scrubbing can also achieve low outlet dust concentrations, indicating that pollutant-removal performance cannot be inferred from the wet–dry distinction alone. Zhao et al. [11] investigated sensible-heat recovery from converter gas, supporting the recovery mechanism represented in S2. These studies provide a basis for interpreting the process differences, rather than directly comparable estimates of their life cycle impacts.

The non-climate screening profiles in Figure 2 do not exhibit a uniform improvement across all categories. Lower utility consumption and greater energy recovery can reduce upstream burdens, whereas filter-media production and substance-specific emissions can introduce additional impacts. The outcome depends on the balance between these contributions within each category. In particular, lower total dust emissions do not necessarily imply proportionate reductions in toxicity-related impacts, which also depend on chemical composition, particle characteristics, and the receiving environmental compartment.

Accordingly, Figure 2 indicates a consistent climate benefit under the central assumptions but a more heterogeneous response across the non-climate categories. The latter are interpreted as screening results for identifying potential burden shifts, rather than as evidence of an overall environmental ranking. Section 3.2 examines the process contributions underlying these differences.

3.2. Process Contributions and Environmental Trade-Offs

Figure 3a separates the common BOFG oxidation burden of 159.008 kg CO_2-eq/FU from the operating inputs and energy credits that distinguish the routes. In their assessment of CO production from BOFG, Hense et al. [20] included the replacement heat needed when gas is redirected to chemical production. Collis et al. [22] likewise accounted for

compensation of the energy service previously supplied by steel mill gas. Retaining both BOFG oxidation and actual energy substitution in the present comparison follows the same principle of functional equivalence. Recovering gas that would otherwise be lost changes the energy service delivered and the amount of external supply displaced. It does not, in these routes, change the ultimate destination of the gas carbon.

For S0, the upstream burden is 6.142 kg CO_2-eq/FU and the BOFG substitution contribution is −46.774 kg CO_2-eq/FU. The corresponding values for S1 are 1.704 and −52.090 kg CO_2-eq/FU. Of the 9.754 kg CO_2-eq/FU saved by moving from S0 to S1, lower upstream demand contributes 4.438 kg CO_2-eq/FU (45.50%) and additional gas recovery contributes 5.315 kg CO_2-eq/FU (54.50%). This decomposition identifies utility efficiency and fuel-gas use as separate sources of the advantage of dry cleaning. A comparison restricted to cleaning electricity would omit the additional energy-substitution benefit.

S2 recovers the same amount of BOFG as S1; its additional climate benefit arises from sensible-heat substitution. Its upstream net burden increases by 0.110 kg CO_2-eq/FU, while 50% useful-heat utilization contributes a credit of −6.428 kg CO_2-eq/FU, reducing net GWP to 102.304 kg CO_2-eq/FU. The direction agrees with the increase in steam generation and improvement in energy performance reported by Zhao et al. [11] when gas–solid separation and a waste-heat boiler replaced evaporative cooling. Both configurations reduce losses of sensible heat from high-temperature off-gas. They nevertheless differ because S2 also introduces PPS filtration, whose material and additional operating requirements must be counted separately. The steam gain measured in that industrial trial cannot therefore be inserted directly as the life cycle emission reduction associated with the present route.

The absolute GWP of S2 remains positive, whereas some BOFG utilization scenarios examined by de Kleijne et al. [19] produced negative net climate impacts. The difference primarily concerns carbon storage and the conditions of system expansion. The negative-result scenarios in that study included CO_2 storage and used conventional product supplies as comparators. Our routes include neither permanent carbon storage nor removal of the eventual oxidation burden, simply because BOFG has been recovered. The different signs are therefore not contradictory findings for an equivalent system. They follow from substantive differences in carbon destination and in the service or product displaced by the alternative route.

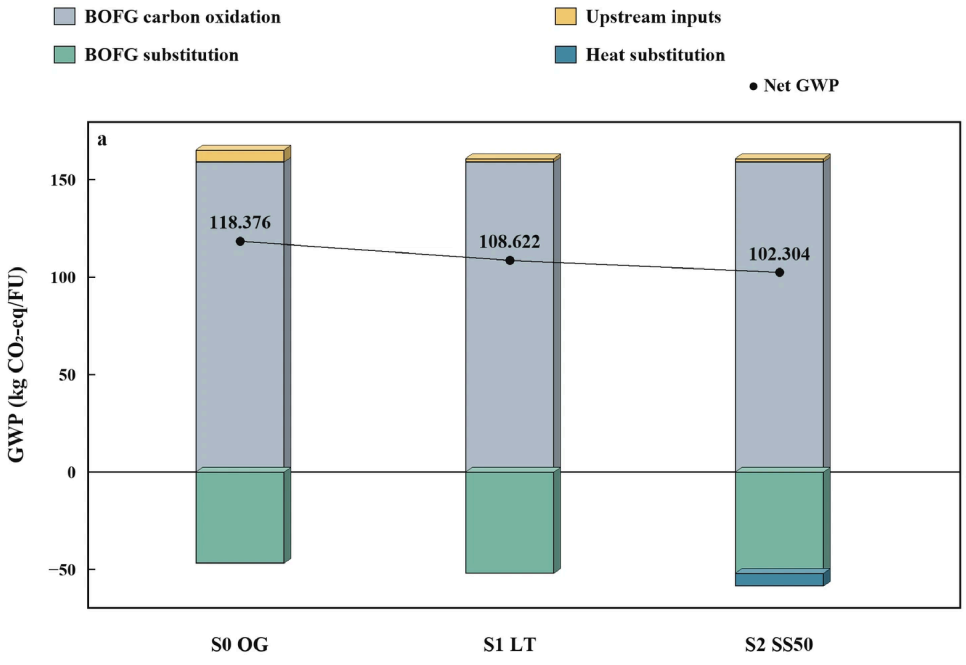


Figure 3. *Cont.*

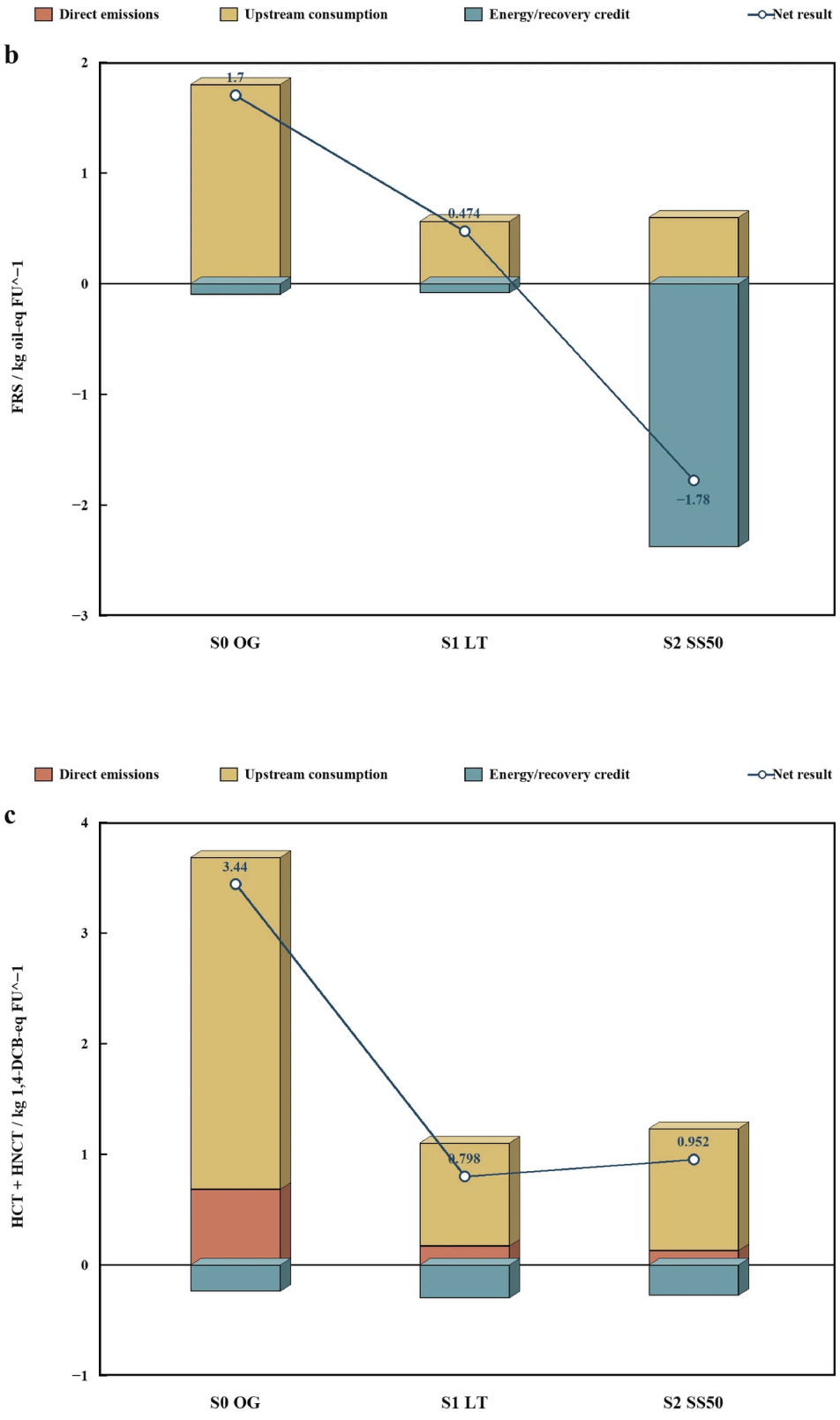


Figure 3. *Cont.*

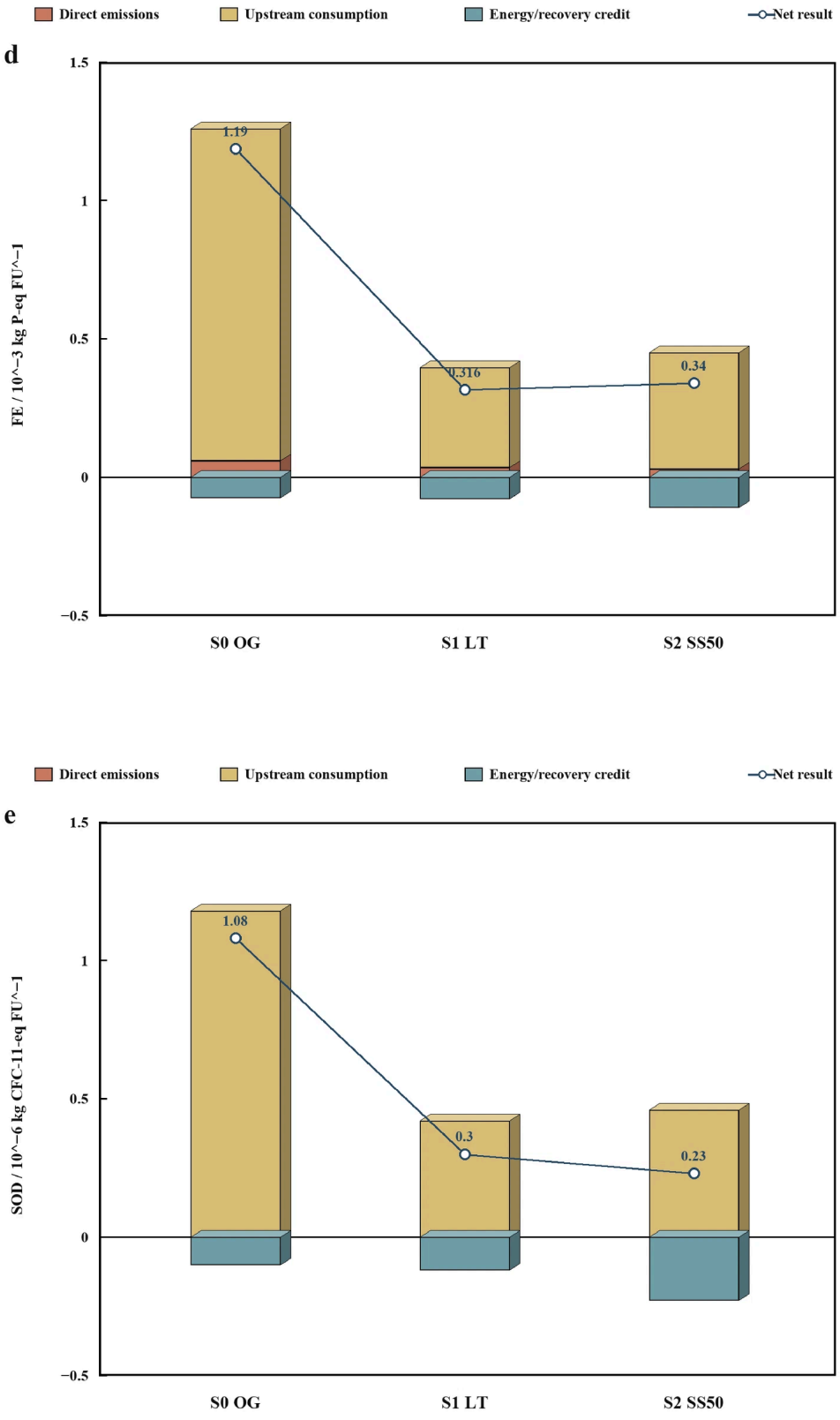


Figure 3. *Cont.*

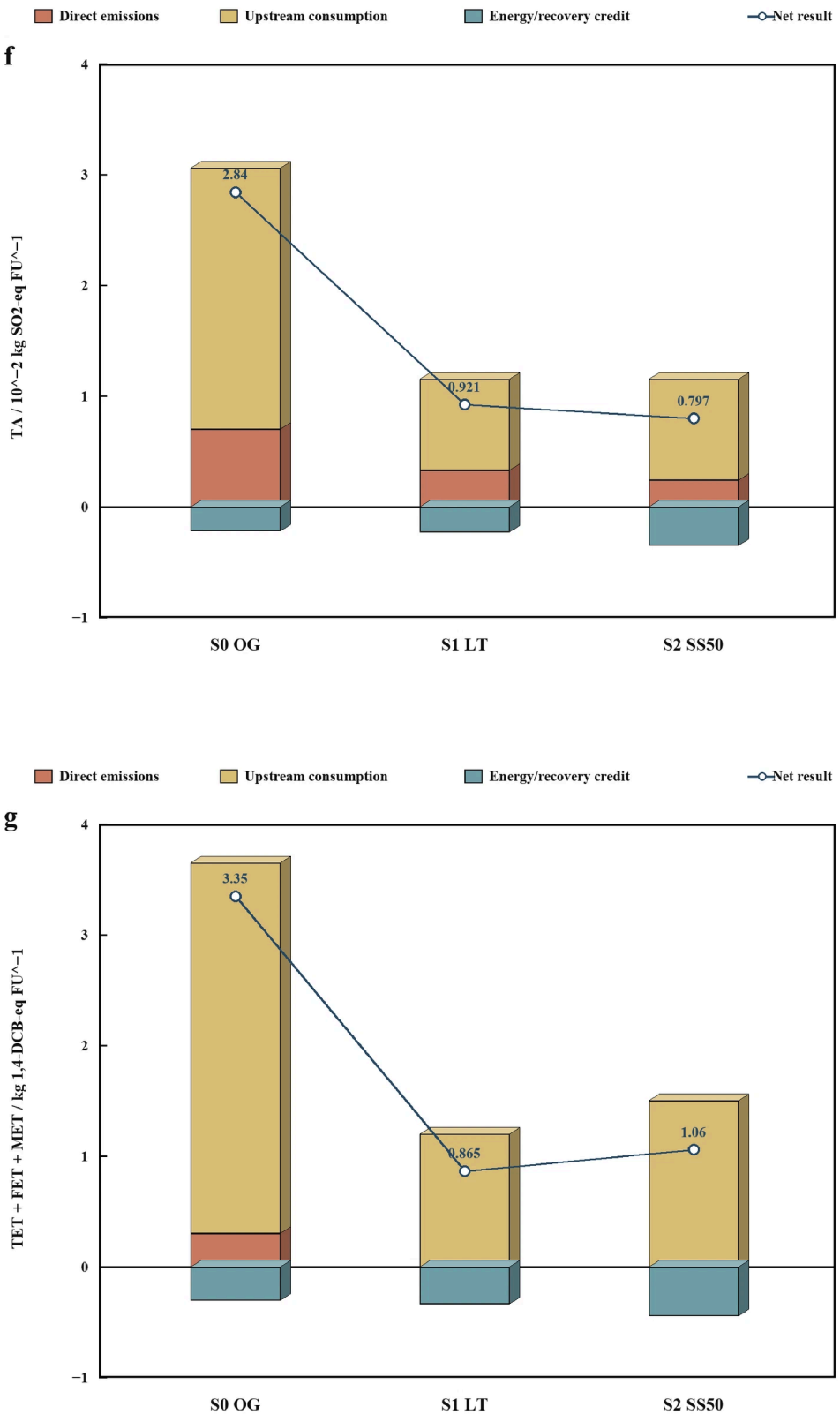


Figure 3. *Cont.*

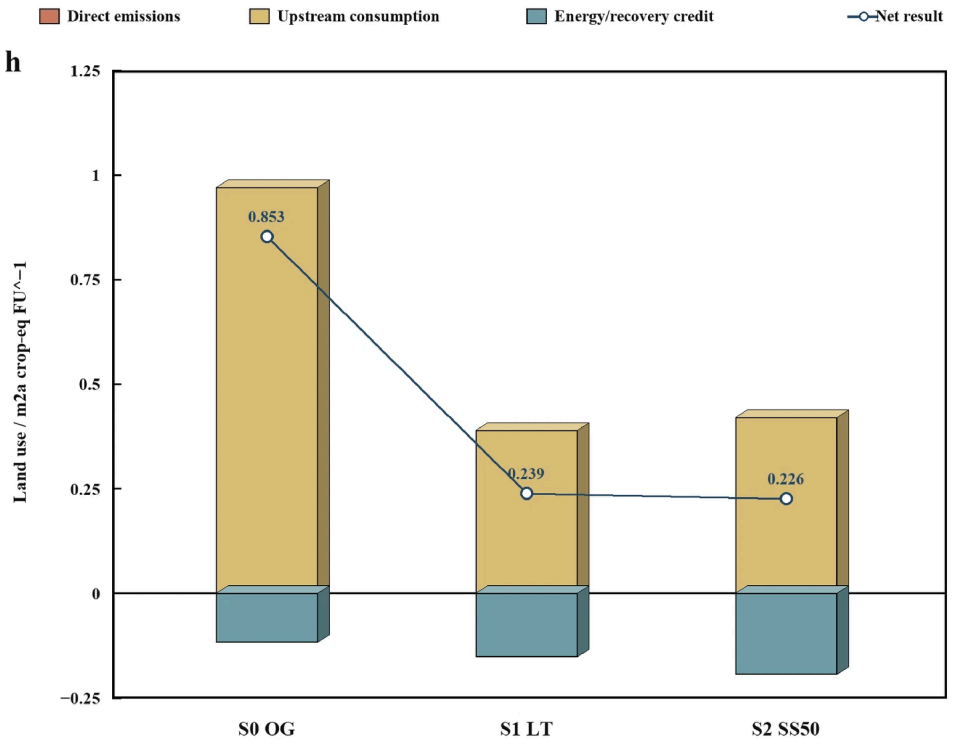


Figure 3. Process contributions for (**a**) GWP; (**b**) FRS; (**c**) the diagnostic sum HCT+HNCT; (**d**) FE; (**e**) SOD; (**f**) TA; (**g**) the diagnostic sum TET+FET+MET; and (**h**) LU. S2 is shown at 50% useful-heat utilization. Panel a separates common BOFG carbon oxidation, upstream burden, BOFG substitution, and useful sensible-heat substitution. Panels (**b**–**h**) retain screening contribution structures, including proxy-dependent splits; their component magnitudes and recovered-solid contributions are not validated quantitative attributions or avoided-product credits. The toxicity sums are display groupings, not additional ReCiPe categories.

Carbon destination also explains why results from solid-waste valorization cannot be transferred directly to sensible-heat recovery. Reddy et al. [29] investigated the effect of BOF-slag particle size on sequestration of landfill-gas CO_2 through carbonation, where carbonate formation provides the storage mechanism. Sensible-heat recovery in S2 contains no comparable carbon-fixation step. Yang et al. [30], comparing incineration, gasification, pyrolysis liquefaction, and hydrothermal liquefaction of antibiotic residues, treated the relevant CO_2 according to the biogenic–carbon boundary and identified energy demands such as drying as important contributors. Fossil BOFG does not meet the same carbon-accounting premise. The transferable insight is that processing inputs and recovered products jointly determine the net burden; neither the carbon convention nor the numerical climate result can be adopted unchanged.

The non-climate screening contribution patterns in Figure 3b–h indicate potential shifts among direct emissions, utilities and material supply. Cui et al. [14] linked the burdens of wet denitrification and ozone oxidation in sintering flue-gas treatment to sodium sulfite, electricity, and liquid oxygen. Although the routes studied here do not use that reaction chain, they share the possibility that additional materials and energy offset part of the benefit from lower on-site emissions. For PPS filtration, extending the filter life reduces the mass of filter material required per functional unit. It need not reduce every toxicity indicator in the same proportion, because the emitted substances, receiving compartments, chemical forms, and characterization factors differ. The proxy-dependent non-climate splits consequently identify potential contributors rather than supporting the same quantitative attribution as the carbon balance in Figure 3a.

Recovered solids face constraints that differ from those governing recovered energy. Lanzerstorfer [7] and Andersson et al. [8] showed that recycling zinc-bearing dust requires control of impurity accumulation and recirculation within the steelworks. Yang et al. [9] further identified the additional energy, reagents, and subsequent pollution control that may be needed for more intensive Zn–Fe separation. Gao et al. [31] recovered Fe, Pb, and Zn from blast-furnace dust through enhanced roasting and magnetic separation, a route that likewise introduces thermal treatment and separation inputs [32]. Capturing an iron-bearing solid therefore does not establish that primary raw-material substitution has occurred [33,34]. In the GWP model in the present study, a captured mass is not automatically assigned a negative product contribution without a defined composition, downstream treatment, product destination, and displaced material [35].

Conversion of a recovered solid into a substitutable product also requires the quality criteria of the intended use to be met. Yang et al. [36], in a bibliometric study of steel slag in road construction, identified reactivity, stability, and carbonation as important research themes. Bulatbekova et al. [37] reviewed the effects of different steelmaking slags on hydration and durability in construction materials, while Wang et al. [38] examined the properties achieved through preparation and modification of gas-quenched steel-slag beads. These studies considered slag rather than BOF dust. Their relevance is the requirement to establish a substitution relationship through material composition, processing and end-use performance together. Without those conditions, product credits cannot be calculated solely from the mass collected by the gas-cleaning system.

3.3. Endpoint Damage and Differences Between Protection Domains

Midpoint impacts and endpoint areas of protection describe different levels of the characterization chain. ReCiPe links substance-specific impact pathways to human health, ecosystems, and resource availability [32]. A reduction in GWP does not establish a corresponding reduction in all endpoint damage pathways, because toxicity, particulate matter formation, acidification, and eutrophication can respond differently to the same process change.

The previously calculated human-health and ecosystem totals were not updated consistently with the complete BOFG carbon inventory. Their absolute values and percentage differences are therefore not reported. Without joint recharacterization, these totals cannot demonstrate that S2 has lower human-health or ecosystem damage than S1. The assessment instead retains the individual midpoint categories to identify the pathways that a consistent endpoint calculation would need to resolve.

Previous BOFG assessments illustrate why climate and health outcomes may diverge. de Kleijne et al. [19] found that the relative performance of BOFG uses depended on the products displaced and the impact category considered. Those routes differ from the cleaning and sensible-heat recovery configurations studied here; so, their endpoint values are not transferred to this assessment. Their relevance is the need to consider the additional processing burdens and the substitution boundary before interpreting an aggregate damage result.

Resource impacts are retained as midpoint screening estimates. Hense et al. [20] reported increased mineral and metal resource consumption in scenarios with lower climate impacts, illustrating that energy-related improvements need not reduce material demand. The incomplete crude-oil-based resources proxy is excluded. Neither the qualitative endpoint discussion nor the normalized midpoint profiles are used to construct an overall ranking of the three treatment routes.

3.4. Category-Level Normalization and Environmental Hotspots

Category-level normalization expresses each midpoint result relative to its World 2010 H annual per-capita reference burden, allowing the magnitudes of different environmental mechanisms to be displayed in PE/FU (Figure 4). Figure 2 emphasizes differences among routes within each category; Figure 4 instead shows the environmental profile of each route against category-specific reference loads. Normalization removes differences in the original physical units but does not assign equal environmental significance to the categories. Equal person-equivalent values in different categories are not interchangeable damages and do not constitute a weighting scheme.

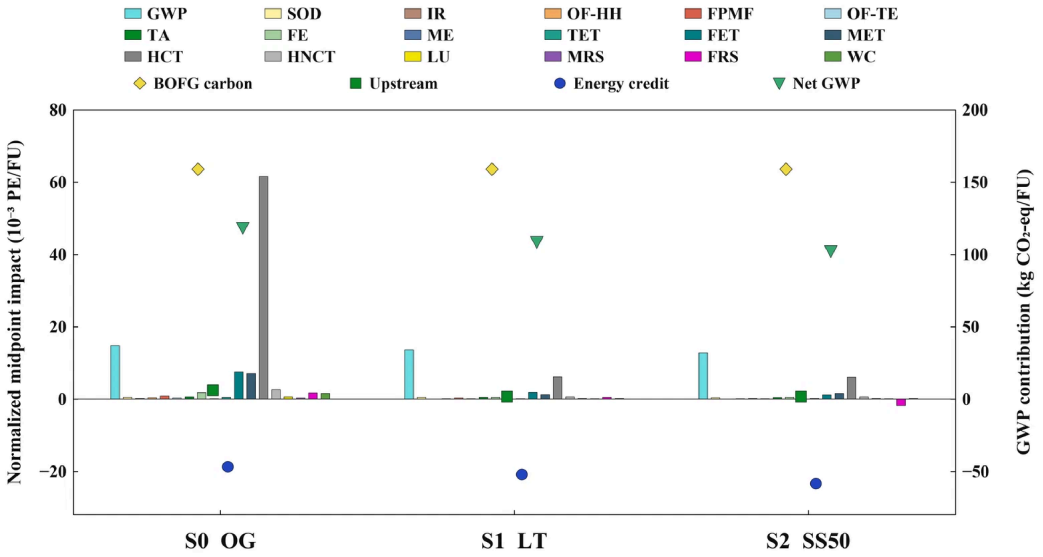


Figure 4. Category-level normalization for S0, S1, and S2-SS50. Colored bars use the left axis (10^{-3} PE/FU) and retain 18 separate categories. GWP is recalculated; the other 17 categories are inherited screening estimates, including proxy-dependent contributions, and do not establish validated multicategory superiority. Symbols use the right axis (kg CO_2-eq/FU) and show common BOFG oxidation, upstream inputs, combined BOFG and sensible-heat substitution credits, and net GWP.

In the retained screening profiles, human carcinogenic toxicity, global warming, and aquatic ecotoxicity have relatively prominent normalized magnitudes for S0. After the transition to S1, GWP becomes more prominent among the remaining burdens. S2 lowers the recalculated climate result further, whereas some screening toxicity and eutrophication estimates do not show a corresponding decrease. These patterns identify candidate priorities for inventory refinement. Because the 17 non-GWP categories were not jointly recharacterized with the revised inventory, their relative magnitudes do not establish measured hotspots or a definitive ranking of treatment routes.

Normalized GWP is 0.0148147, 0.0135941, and 0.0128034 PE/FU for S0, S1, and S2-SS50, respectively. The same normalization factor is applied to all three routes, so the reductions of 8.24% and 5.82% are unchanged. The negative FRS value retained for S2 belongs to the screening model and cannot independently validate the magnitude of a resource-substitution credit. In general, a negative net category result means that modeled avoided burdens exceed modeled inputs within that category; it does not demonstrate atmospheric carbon removal or a negative total environmental burden.

Benini and Sala [39] showed through sensitivity analysis that normalization factors can be affected by the reference emissions inventory, elementary-flow mapping, emission compartments, and regional characterization assumptions. The ReCiPe World reference used here differs from the ILCD European reference examined in their study. Their factors and uncertainty magnitudes are therefore not transferred to this analysis. Instead, their

findings inform the interpretation of our normalized profiles; a hotspot results from the foreground inventory and the chosen reference system together. Its height is not a direct ranking of measured pollutant hazard, and changes in the reference inventory can affect the relative prominence of categories even when the treatment inventory remains unchanged.

All 18 PE/FU results are retained separately. An unweighted sum would implicitly assign equal importance to different impact mechanisms and allow their positive and negative values to cancel. It cannot provide a justified overall ordering of the routes. The right axis of Figure 4 reports only the GWP contributions, in kg CO_2-eq/FU. These symbols connect the normalized profiles to the climate balance; they are not an aggregate environmental score.

Potential material-related hotspots in the normalized profile ultimately need to be resolved through pollutant speciation and fate. Yang et al. [40] examined Pb(II) and Cd(II) adsorption on modified coal-gasification slag together with competitive adsorption, leaching toxicity, and adsorption mechanisms. That combination illustrates why material function and environmental safety require separate assessment. The material studied was neither BOF dust nor PPS;, its adsorption performance cannot establish the toxicity of the materials considered here. Its methodological relevance lies in the attention paid to metal form, release behavior and final destination. Together with the burdens of treatment inputs identified by Cui et al. [14], this supports using the present non-climate hotspots to prioritize characterization of material service life and substance-specific releases.

The quantitative climate result suggests useful sensible-heat recovery under the stated substitution conditions. Filter life, pollutant speciation, wastewater composition, and the actual destination of captured solids remain priorities for resolving the non-climate pathways. Category-level normalization identifies where further characterization is needed; it does not remove the uncertainty of the underlying inventory or establish comprehensive environmental superiority.

3.5. Sensitivity and the Conditions for Additional Climate Benefit

The GWP response of each route depends on both operating parameters and the external energy displaced by recovery, but these two influences do not act identically on absolute burdens and differences between routes. Figure 5a–c shows the response of S0, S1, and S2 to parameter-specific low and high inputs relative to their respective central cases. Reducing the GWP factor for displaced useful heat lowers the substitution credit per unit of recovered energy and therefore raises the absolute GWP of all three routes. Across the displaced-heat scenario range of 0.0500–0.1000 kg CO_2-eq/MJ, the factor produces changes of −14.20% to +12.66% for S0, −17.23% to +15.36% for S1, and −20.55% to +18.32% for S2. The wider response of S2 arises because the same factor applies to both BOFG and sensible-heat credits. Its climate performance is consequently more exposed to the carbon intensity of the displaced heat supply.

This direction agrees with the finding of de Kleijne et al. [19] that grid decarbonization weakens the substitution benefit of electricity generated from BOFG; the cleaner the displaced supply, the smaller the avoided burden for a given amount of recovered energy. By contrast, the clean-electricity and electrolytic-hydrogen scenarios examined by Hense et al. [20] can lower the burden of processing BOFG into CO. Lowering the carbon intensity of energy consumed by a process and lowering that of the energy displaced by the process are therefore different changes. In our system, the first reduces operating emissions, whereas the second reduces the credits assigned to BOFG and sensible-heat recovery. Treating them as one undifferentiated background-energy effect would obscure their opposing contributions to net GWP.

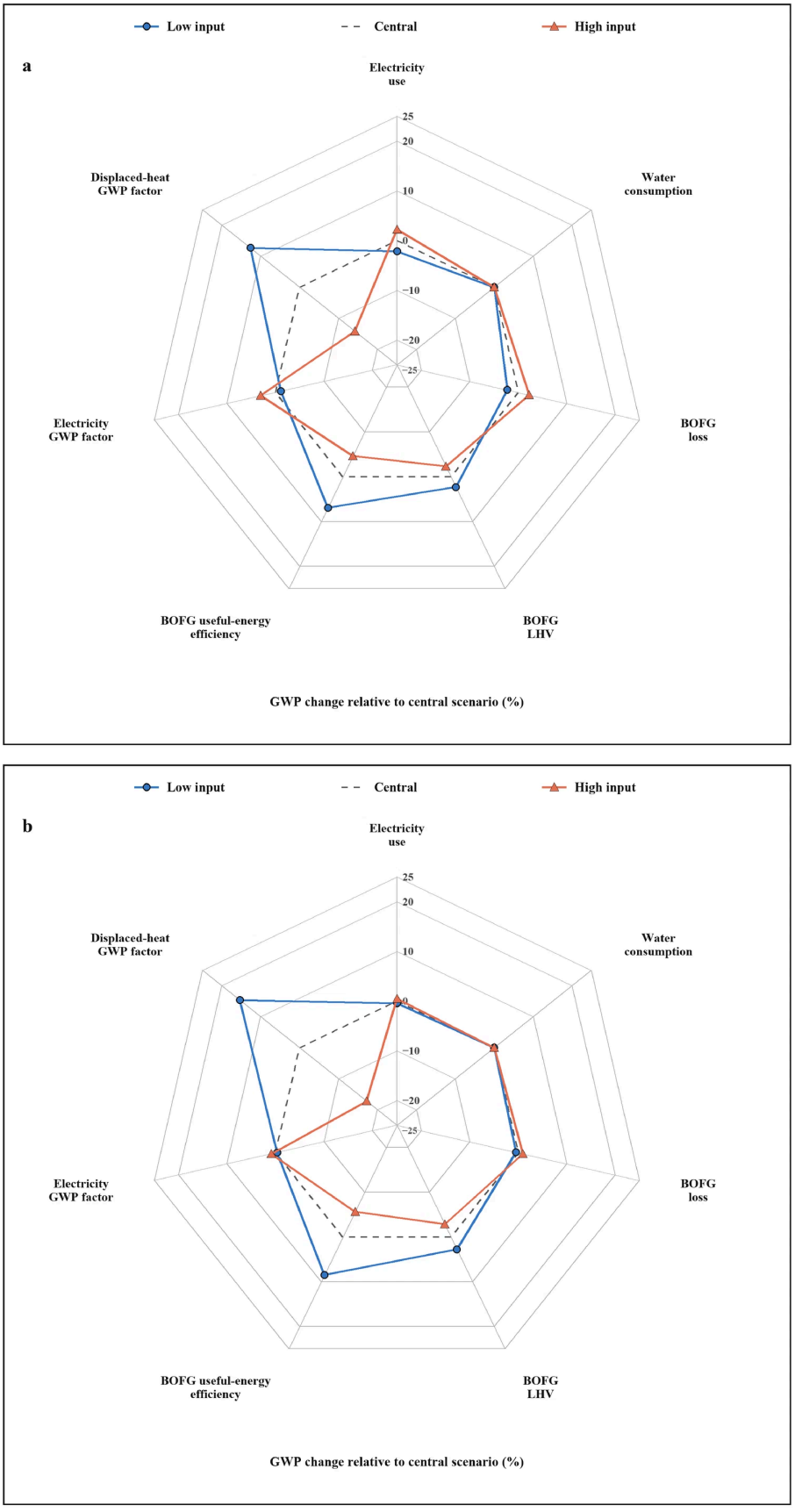


Figure 5. *Cont*.

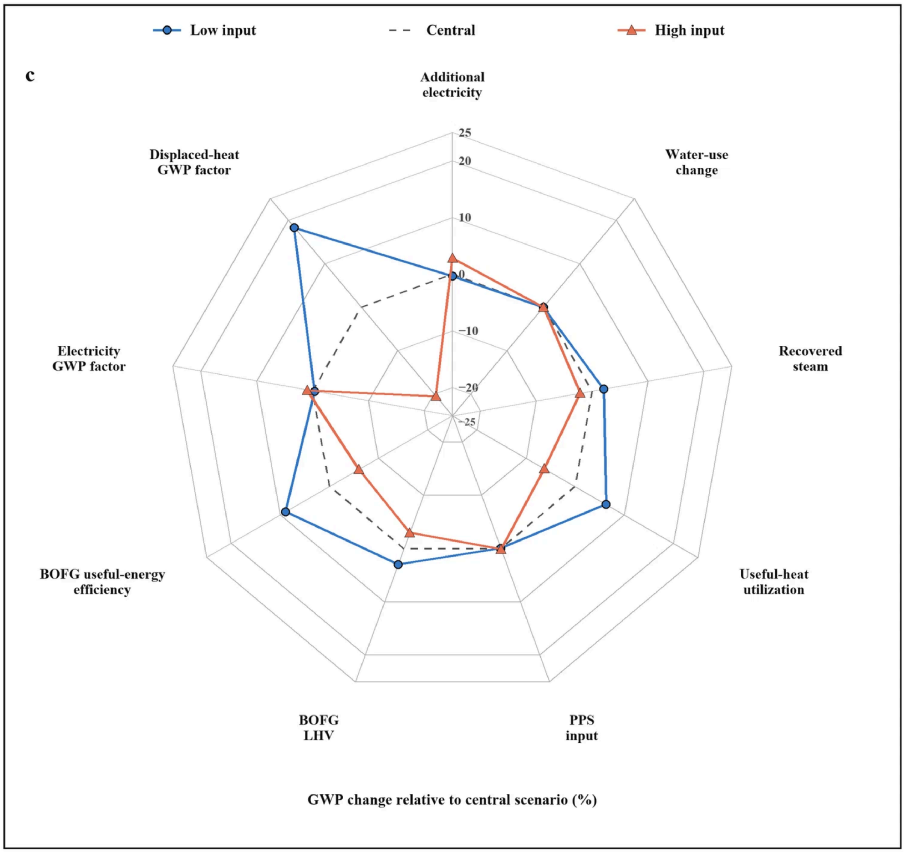


Figure 5. Deterministic one-factor-at-a-time sensitivity of GWP for (**a**) S0, (**b**) S1, and (**c**) S2. Radial values are percentage changes from each route's central GWP; the dashed polygon denotes zero change. Blue circles and red triangles correspond to low and high parameter inputs, not necessarily low and high GWP outcomes. One parameter is varied at a time; the central S2 case uses 50% useful-heat utilization. Shared energy factors are applied consistently.

The operating responses also distinguish wet and dry treatment. Varying S0 electricity consumption from 6.0 to 15.0 kWh/FU changes GWP by ±2.20% around the central result. For S1, the range of 2.0–3.8 kWh/FU gives a response of ±0.48%. This contrast reflects both the electricity demand of each route and the width of its specified input range. In S2, lowering useful-heat utilization from the central 50% to 0% increases GWP by 6.28%, whereas raising utilization to 100% decreases it by 6.28%. PPS input and changes in water consumption produce smaller GWP responses within the tested bounds. However, a small climate response does not imply that filtration materials are negligible with regard to toxicity, resource scarcity, or final disposal. Those mechanisms require assessment through their own impact pathways rather than inference from the GWP sensitivity alone.

The scale of the energy-efficiency gain in S2 must also be distinguished from reductions achieved by changing the principal steelmaking process. Bhardwaj et al. [41] used material and energy balances for a large Indian steelworks to assess decarbonization options and emphasized interactions among process units. Kildahl et al. [42] proposed thermochemical coupling to change the carbon cycle of a blast furnace–BOF system. Such interventions alter the main reductant or the conversion of carbon through the plant. Our comparison instead holds BOFG generation and composition constant. The smaller incremental reductions reported here therefore do not contradict the potential of deeper process transformation; they reflect a different retrofit target and a narrower system boundary.

S1 and S2 have the same BOFG generation, composition, and recovered volume. Their common carbon-oxidation burden and gas-substitution credit consequently cancel in a

paired comparison. The incremental climate effect of S2 is determined by the difference between its additional utility and PPS burdens and the credit for useful sensible heat. Expressing this difference explicitly separates the consequences of adding heat recovery from the carbon and energy terms already present in the dry LT reference:

$$\Delta GWP_{2-1} = \Delta E f_E + \Delta W f_W + m_{PPS} f_{PPS} - m_{st} \Delta h \, u \, f_H$$

where ΔE and ΔW are the changes in electricity and industrial-water use from S1 to S2; m_{PPS} is the PPS input; mst is recovered steam mass; Δh is the steam enthalpy increase; and u is the useful-heat utilization ratio. The factors f_E, f_W, f_{PPS}, and f_H characterize electricity, industrial water, PPS, and displaced useful heat, respectively. The expression covers the operating inputs and energy substitution included in the model. It does not include the embodied burdens of manufacturing the heat-recovery equipment or its supporting infrastructure; the resulting threshold applies to this stated boundary.

Under central parameters, the additional upstream net burden is 0.110126175 kg CO_2-eq/FU and full utilization of the recoverable heat provides a substitution credit of 12.855990741 kg CO_2-eq/FU. The relationship is therefore $\Delta GWP_{2-1} = 0.110126175 - 12.855990741u$. At useful-heat utilization ratios of 0%, 25%, 50%, 75%, and 100%, the absolute GWP of S2 is 108.732, 105.518, 102.304, 99.090, and 95.876 kg CO_2-eq/FU, respectively. The corresponding differences from S1 are +0.110, −3.104, −6.318, −9.532, and −12.746 kg CO_2-eq/FU. Without effective heat substitution, the additional filtration inputs leave S2 slightly above S1. As more of the recovered heat displaces an external supply, the incremental climate benefit increases linearly under fixed background factors. The five modeled cases are reported in Table S2.

The zero sensible-heat-credit case isolates dependence on external heat displacement while retaining the same BOFG use as S1 and S2. With no credit for the additional recovered heat, S2 exceeds S1 by 0.110 kg CO_2-eq/FU under central operation and by 3.082 kg CO_2-eq/FU under the adverse operating combination with central electricity. Recovering heat without replacing an external supply therefore does not generate the climate saving attributed to useful-heat substitution.

Parameters that strongly affect absolute GWP do not necessarily control the difference between S2 and S1. If both routes use the same recovered gas volume and energy parameters, the BOFG lower heating value and useful-energy efficiency can substantially change their individual absolute results without changing the paired difference. By contrast, useful-heat utilization, steam production, additional electricity, and the carbon intensity of displaced heat act directly on the incremental result. Distinguishing these responses prevents uncertainty in the shared energy system from being mistaken for an advantage or risk specific to S2. It also indicates why the parameters most influential in an absolute-GWP radar plot need not be the first priorities for optimizing the heat-recovery retrofit.

The industrial trial by Zhao et al. [11] established an engineering basis for increasing recoverable steam. Our incremental model shows that the life cycle benefit depends on steam output multiplied by the fraction that is effectively used, under the specified steam enthalpy and displaced-heat factor. The gas–steam–electricity network analysis by Qiu et al. [23] and the assessment of staged integrated-steelworks retrofits by Onarheim and Arasto [43] both show that by-product energy use is linked to the plant's wider energy supply. BOF heat is generated intermittently. Increased heat-transfer capacity therefore produces sustained substitution only when it is matched to heat-user demand, the required steam grade, and the timing of supply and consumption. Recoverable heat at the process outlet and energy actually displaced by the user cannot be treated as equivalent quantities.

If BOFG is diverted to chemicals, the assessment must expand to include additional separation and reaction stages. Oh et al. [44] combined experiments, simulation, and techno-economic analysis of CO production from BOFG, showing that bed configuration and target

purity jointly affected the separation scheme. Bashir et al. [45], studying pressure-swing recovery of H_2, CO, and CO_2 from steel mill gases, likewise examined constraints involving product purity, recovery, and cost. Javan-Bari et al. [46] simulated liquid-hydrocarbon production from combined blast-furnace and coke oven gases, while Ling et al. [47] analyzed the thermodynamic feasibility of methanating steelworks by-product gases. All these routes extend beyond the heat-substitution boundary used here. The heat credit in this model cannot simply be replaced by a credit for a higher-value chemical without also adding the associated processing inventory and specifying the conventional product supply that is displaced.

S2 reaches climate break-even relative to S1 when $\Delta GWP2{-}1 = 0$. The central critical useful-heat utilization ratio is 0.86%. This low value mainly reflects the absence of additional electricity demand in the central S2 case and the partial offset of its PPS burden by reduced water use. Under a joint operating case with 5.0 kWh/FU of additional electricity, no extra water saving, 0.0255 kg/FU of PPS, and only 50 kg/FU of recovered steam, the threshold rises to 35.96%. That calculation holds the electricity and natural-gas useful-heat factors at 0.5777 kg CO_2-eq/kWh and 0.073567901 kg CO_2-eq/MJ, respectively. At 50% utilization, this operating combination still reduces GWP by 1.203 kg CO_2-eq/FU relative to S1. The conclusion is conditional on those background factors and should not be generalized to a different displaced heat supply or electricity mix.

Joint changes in the energy background can reverse that result. For the same additional-input combination, reducing the useful-heat factor to 0.0500 kg CO_2-eq/MJ raises the critical utilization ratio to 52.92%. If the electricity factor simultaneously increases to 0.9240 kg CO_2-eq/kWh, the threshold reaches 82.64%. S2 at 50% utilization then exceeds S1 by 1.901 kg CO_2-eq/FU. These results are deterministic combinations within the stated scenario bounds. They show that 50% utilization is not a general guarantee of further decarbonization across energy backgrounds and that 35.96% is not the highest possible threshold among all allowed combinations. Joint probability distributions and information on operating correlations are not available in the model. The boundary cases therefore identify conditions under which the advantage can reverse; they do not estimate the probability of that reversal.

Equipment manufacture could reduce the operating-stage advantage of S2 if its additional heat-recovery and filtration equipment has a positive net embodied burden after accounting for equipment displaced from S1. Let $\Delta Gcap$ denote that net burden allocated per FU over the relevant service lives and throughput. Under central operation, the incremental result becomes $\Delta GWP_{2-1} = 0.110126175 + \Delta Gcap - 12.855990741u$. At 50% useful-heat utilization, the central operating benefit can accommodate a net embodied burden of up to 6.318 kg CO_2-eq/FU before break-even. The corresponding allowance is only 1.203 kg CO_2-eq/FU under the adverse operating combination with central energy factors. These are analytical allowances, not estimates of actual equipment manufacture.

Even at 100% useful-heat utilization, S2 retains an absolute GWP of 95.876 kg CO_2-eq/FU under the central energy background. Heat substitution does not offset the common burden arising from eventual BOFG oxidation. S2 should therefore be understood as an option for an additional reduction conditional on useful heat displacement, not as a route to absolute net-zero or negative-emission off-gas treatment. A retrofit decision must consider the heat that can be consumed sustainably, the additional electricity requirement and the carbon intensity of the heat source actually replaced. Its performance across environmental categories also depends on the non-climate characterization and endpoint pathways; the climate break-even calculation alone cannot establish a comprehensive environmental advantage.

Further reduction of the common carbon burden requires a change in carbon conversion or the addition of capture and storage, rather than heat recovery alone. Zecca et al. [48] investigated CO_2 mitigation by coupling steelworks gas allocation with capture technologies. Xie et al. [49] conducted a pilot study of chemical CO_2 absorption for a top-gas-recycling oxygen blast furnace, examining regeneration energy and process improvements. The first of these issues relates to reconfiguration of plant-wide energy and capture systems; the second concerns blast-furnace recycle gas. Both differ from the cleaning and heat-exchange functions of S2. Any extension of the present study to carbon capture would need to include solvent demand, regeneration heat, compression, and final carbon fate, and to re-establish the boundary required for a functionally equivalent comparison.

4. Conclusions

Wet OG cleaning, dry LT cleaning, and sensible-heat recovery with PPS filtration have central GWPs of 118.376, 108.622, and 102.304 kg CO_2-eq/FU, respectively, with S2 evaluated at 50% useful-heat utilization. The 8.24% reduction from S0 to S1 arises from lower utility burdens and greater BOFG recovery, contributing 45.50% and 54.50% of the saving. S2 provides a further reduction of 6.318 kg CO_2-eq/FU through useful sensible-heat substitution. Its break-even utilization is 0.86% under central assumptions, 35.96% under adverse operation with central energy factors, and 82.64% under a jointly adverse operating and energy-background scenario. These are deterministic conditions dependent on the adopted background proxies, not probabilities or universal technology thresholds. Even at full heat utilization, S2 retains a positive GWP of 95.876 kg CO_2-eq/FU. The 17 non-climate screening categories indicate possible burden shifts but do not establish comprehensive environmental superiority. Quantitative endpoint rankings are withheld pending consistent characterization. Site-specific decisions should test actual heat demand, additional electricity use, steam performance, filter replacement, and substance-specific emissions against the stated carbon and substitution boundaries.

Supplementary Materials: The following supporting information can be downloaded at: https://www.mdpi.com/article/10.3390/pr14213388/s1, Table S1: Parameter ranges and GWP responses for the one-factor-at-a-time sensitivity analysis; Table S2: Absolute GWP of S2 and its difference from S1 at different useful-heat utilization ratios; Table S3: Climate break-even thresholds for S2 under combined operating and energy-background scenarios; Table S4: Sources and limitations of inventory inputs and GWP characterization factors; Table S5: Central GWP contributions of the three BOF off-gas treatment routes. The Supplementary Materials also include additional methodological details on useful-heat utilization scenarios, deterministic joint boundary cases, input sources and characterization scope, central GWP balance and boundary checks, and background-factor derivation and additional checks.

Author Contributions: Conceptualization, J.S.; data curation, J.S.; formal analysis, J.S. and J.Y.; software, J.S. and J.Y.; resources and supervision, X.T.; funding acquisition, D.B. and X.Z.; investigation, H.B., D.A., G.Z., M.L. and Y.G.; writing, J.S. and J.Y. All authors have read and agreed to the published version of the manuscript.

Funding: This research was supported by the State Key Laboratory Special Programs of China Minmetals Corporation (2024GZGJ02), and the National Natural Science Foundation of China (No. 52500222).

Data Availability Statement: The inputs and factors needed to reproduce the GWP calculations are provided in Tables 1 and 2, Supplementary Tables S1–S5 and Supplementary Section S6. The non-climate figures retain screening estimates and are not presented as a complete, independently reproducible substance-level LCIA dataset.

Conflicts of Interest: Authors Jian Sun, Dehai Bai, Xiaohua Zhu, Mengxin Li and Jian Yang were employed by the Central Research Institute of Building and Construction Co., Ltd., MCC Group. Authors Xiangang Tang, Hongjuan Bai, Dengfei An and Guangwen Zhou were employed by Energy Saving and Environmental Protection Co., Ltd. The remaining author declares no commercial or financial relationships that could be construed as a potential conflict of interest.

References

1. Pang, Z.; Bu, J.; Yuan, Y.; Zheng, J.; Xue, Q.; Wang, J.; Guo, H.; Zuo, H. The low-carbon production of iron and steel industry transition process in China. *Steel Res. Int.* **2024**, *95*, 2300500. [CrossRef]
2. Kim, S.-W.; Yi, S.-H.; Han, J.-W. A comparative study on environmentally friendly ironmaking process through air to oxygen. *Ironmak. Steelmak.* **2026**, *53*, 639–655. [CrossRef]
3. Gao, J.; Wang, B.; Teng, F.; Qi, Y.; Zhang, Y. Analysis of carbon emission reduction capacity of hydrogen-rich oxygen blast furnace based on renewable energy hydrogen production. *High Temp. Mater. Process.* **2024**, *43*, 20240050. [CrossRef]
4. Yu, J.; Xu, R.; Zhang, J.; Zheng, A. A review on reduction technology of air pollutant in current China's iron and steel industry. *J. Clean. Prod.* **2023**, *414*, 137659. [CrossRef]
5. Li, Z.; Zhu, R.; Ma, G.; Wang, X. Laboratory investigation into reduction the production of dust in basic oxygen steelmaking. *Ironmak. Steelmak.* **2017**, *44*, 601–608. [CrossRef]
6. Li, X.; Tang, P.; Jiang, J.; Fu, Q.; Wen, G. Control of zinc-containing dust agglomerates in basic oxygen furnace flue gas cleaning system. *ISIJ Int.* **2021**, *61*, 763–772. [CrossRef]
7. Lanzerstorfer, C. Zinc enrichment in in-plant electrostatic precipitator dust recycling by air classification in converter steelmaking. *Steel Res. Int.* **2019**, *90*, 1800377. [CrossRef]
8. Andersson, A.; Gullberg, A.; Kullerstedt, A.; Sandberg, E.; Andersson, M.; Ahmed, H.; Sundqvist-Ökvist, L.; Björkman, B. A holistic and experimentally-based view on recycling of off-gas dust within the integrated steel plant. *Metals* **2018**, *8*, 760. [CrossRef]
9. Yang, J.; Wang, H.; Du, Y.; Jiao, L.; Wang, W.; Zhang, W.; Ma, H. A classification-based decision framework for valorizing zinc-bearing metallurgical dusts. *Miner. Eng.* **2026**, *247*, 110516. [CrossRef]
10. Xu, J.; Bao, X.; Chen, G.; Lv, L. A novel process for ultra-low emission of flue gas by adding waste heat steam. *Sep. Purif. Technol.* **2024**, *335*, 126158. [CrossRef]
11. Zhao, J.; Li, B.; Wei, X.; Li, T.; Li, S. New green and low-carbon technology for all-sensible heat recovery of converter gas. *J. Clean. Prod.* **2024**, *438*, 140699. [CrossRef]
12. Chen, L.; Shen, X.; Xia, S.; Sun, F. Thermodynamic analyses for recovering residual heat of high-temperature basic oxygen gas (BOG) by the methane reforming with carbon dioxide reaction. *Energy* **2017**, *118*, 906–913. [CrossRef]
13. Yang, L.-Z.; Jiang, T.; Li, G.-H.; Guo, Y.-F.; Chen, F. Present situation and prospect of EAF gas waste heat utilization technology. *High Temp. Mater. Process.* **2018**, *37*, 357–363. [CrossRef]
14. Cui, L.; Ba, K.; Li, F.; Wang, Q.; Ma, Q.; Yuan, X.; Mu, R.; Hong, J.; Zuo, J. Life cycle assessment of ultra-low treatment for steel industry sintering flue gas emissions. *Sci. Total Environ.* **2020**, *725*, 138292. [CrossRef] [PubMed]
15. Cui, L.; Liu, M.; Yuan, X.; Wang, Q.; Ma, Q.; Wang, P.; Hong, J.; Liu, H. Environmental and economic impact assessment of three sintering flue gas treatment technologies in the iron and steel industry. *J. Clean. Prod.* **2021**, *311*, 127703. [CrossRef]
16. Uribe-Soto, W.; Portha, J.-F.; Commenge, J.-M.; Falk, L. A review of thermochemical processes and technologies to use steelworks off-gases. *Renew. Sustain. Energy Rev.* **2017**, *74*, 809–823. [CrossRef]
17. Lee, J.-K.; Lee, I.-B.; Han, J. Techno-economic analysis of methanol production from joint feedstock of coke oven gas and basic oxygen furnace gas from steel-making. *J. Ind. Eng. Chem.* **2019**, *75*, 77–85. [CrossRef]
18. Bampaou, M.; Panopoulos, K.; Seferlis, P.; Voutetakis, S.; Matino, I.; Petrucciani, A.; Zaccara, A.; Colla, V.; Dettori, S.; Branca, T.A.; et al. Integration of renewable hydrogen production in steelworks off-gases for the synthesis of methanol and methane. *Energies* **2021**, *14*, 2904. [CrossRef]
19. de Kleijne, K.; James, J.; Hanssen, S.V.; van Zelm, R. Environmental benefits of urea production from basic oxygen furnace gas. *Appl. Energy* **2020**, *270*, 115119. [CrossRef]
20. Hense, J.; Bachmann, M.; Polte, L.; von der Aßen, N.; Jupke, A. Integrated process design and life cycle assessment of carbon monoxide provision from basic oxygen furnace gas. *Chem. Ing. Tech.* **2022**, *94*, 1524–1535. [CrossRef]
21. Eichwald, S.; Polte, L.; Hense, J.; Nilges, B.; Jupke, A.; von der Assen, N. Integrated phosgene and steel production: Combining process optimization and life cycle assessment to minimize greenhouse gas emissions. *Chem. Ing. Tech.* **2024**, *96*, 1256–1267. [CrossRef]
22. Collis, J.; Strunge, T.; Steubing, B.; Zimmermann, A.; Schomäcker, R. Deriving economic potential and GHG emissions of steel mill gas for chemical industry. *Front. Energy Res.* **2021**, *9*, 642162. [CrossRef]

23. Qiu, Z.; Yuan, Y.; Yan, T.; Na, H.; Sun, J.; Wang, Y.; Du, T. Optimization of gas–steam–electricity network of typical iron and steel enterprise. *J. Sustain. Metall.* **2022**, *8*, 806–814. [CrossRef]
24. Yang, J.; Wang, H.; Du, Y.; Wang, H.; Jiao, L.; Yang, S.; Xing, Y.; Ma, H. Life-cycle environmental trade-offs of steel slag treatment processes: A comparative assessment with process-level drivers. *Processes* **2026**, *14*, 1871. [CrossRef]
25. Arvidsson, R.; Tillman, A.-M.; Sandén, B.A.; Janssen, M.; Nordelöf, A.; Kushnir, D.; Molander, S. Environmental assessment of emerging technologies: Recommendations for prospective LCA. *J. Ind. Ecol.* **2018**, *22*, 1286–1294. [CrossRef]
26. Azimi, A.; van der Spek, M. Prospective life cycle assessment suggests direct reduced iron is the most sustainable pathway to net-zero steelmaking. *Ind. Eng. Chem. Res.* **2025**, *64*, 3871–3885. [CrossRef] [PubMed]
27. Tenhumberg, N. EU regulatory compliance of renewable fuels from steel mill gases and exhaust gases. *Chem. Ing. Tech.* **2024**, *96*, 1299–1309. [CrossRef]
28. Department for Energy Security and Net Zero. *Greenhouse Gas Reporting: Conversion Factors 2025*; Full Set and Methodology; UK Government: London, UK, 2025. Available online: https://www.gov.uk/government/publications/greenhouse-gas-reporting-conversion-factors-2025 (accessed on 15 October 2026).
29. ecoinvent. Change Report: Ecoinvent Version 3.10; ecoinvent: Zurich, Switzerland, 2023; Table 76, p. 120. Available online: https://support.ecoinvent.org/hubfs/Knowledge%20Base/Database/Releases/Change%20Report%20v3.10%20-%2020231214.pdf (accessed on 15 October 2026).
30. Touré, A.; Duchet Rumeau, J.; Thollet, B.; Pantaleao, E.; Sautel, J.; Njakou Djomo, S. Environmental impacts of three high-performance thermoplastics (HPTPs) and associated glass-fiber reinforced grades from different processing technologies. *RSC Sustain.* **2026**, *4*, 972–986. [CrossRef]
31. Ministry of Ecology and Environment of the People's Republic of China. 2024 Electricity Carbon Footprint Factors; Tables 1 and 2; 2025. Available online: https://www.mee.gov.cn/xxgk2018/xxgk/xxgk01/202510/W020251024569470952545.pdf (accessed on 15 October 2026).
32. Huijbregts, M.A.J.; Steinmann, Z.J.N.; Elshout, P.M.F.; Stam, G.; Verones, F.; Vieira, M.; Zijp, M.; Hollander, A.; van Zelm, R. ReCiPe2016: A harmonised life cycle impact assessment method at midpoint and endpoint level. *Int. J. Life Cycle Assess.* **2017**, *22*, 138–147. [CrossRef]
33. Reddy, K.R.; Gopakumar, A.; Rai, R.K.; Kumar, G.; Chetri, J.K.; Grubb, D.G. Effect of basic oxygen furnace slag particle size on sequestration of carbon dioxide from landfill gas. *Waste Manag. Res.* **2019**, *37*, 469–477. [CrossRef] [PubMed]
34. Yang, J.; Wei, Y.; Ma, R.; Ma, H.; Dong, B.; Wang, Y. Comparison of thermochemical conversion processes for antibiotic residues: Insights from life cycle assessment. *Processes* **2025**, *13*, 1139. [CrossRef]
35. Gao, C.; Yang, H.; Xu, J.; Sai, M. Recovery of Fe, Pb and Zn from blast furnace gas ash by intensive calcination and magnetic separation techniques. *Separations* **2026**, *13*, 10. [CrossRef]
36. Yang, J.; Ma, R.; Dong, B.; Ma, H.; Wang, Y.; Gao, M.; Sun, Y.; Jin, Y. Research progress and hotspots of steel slag application in road construction: A bibliometric perspective. *Infrastructures* **2025**, *10*, 54. [CrossRef]
37. Bulatbekova, D.; Vashistha, P.; Kim, H.-K.; Pyo, S. Effects of basic-oxygen furnace, electric-arc furnace, and ladle furnace slags on the hydration and durability properties of construction materials: A review. *J. Build. Eng.* **2024**, *92*, 109670. [CrossRef]
38. Wang, H.; Zhang, W.; Liu, C.; Xing, H.; Guo, C.; Zhang, Y. Preparation and performance analysis of gas-quenched steel slag beads. *Metall. Res. Technol.* **2020**, *117*, 105. [CrossRef]
39. Benini, L.; Sala, S. Uncertainty and sensitivity analysis of normalization factors to methodological assumptions. *Int. J. Life Cycle Assess.* **2016**, *21*, 224–236. [CrossRef]
40. Yang, J.; Liu, T.; Ma, R.; Ma, H.; Dong, B.; Xia, C.; Li, H. Adsorption of Pb(II) and Cd(II) on modified coal gasification slag: Competitive adsorption, leaching toxicity, and adsorption mechanism. *ChemistrySelect* **2024**, *9*, e202402909. [CrossRef]
41. Bhardwaj, N.; Seethamraju, S.; Bandyopadhyay, S. Carbon abatement options for large iron and steel plants in India. *J. Clean. Prod.* **2025**, *486*, 144505. [CrossRef]
42. Kildahl, H.; Wang, L.; Tong, L.; Ding, Y. Cost effective decarbonisation of blast furnace–basic oxygen furnace steel production through thermochemical sector coupling. *J. Clean. Prod.* **2023**, *389*, 135963. [CrossRef]
43. Onarheim, K.; Arasto, A. Staged implementation of alternative processes in an existing integrated steel mill for improved performance and reduced CO_2 emissions–Part I: Technical concept analysis. *Int. J. Greenh. Gas Control* **2016**, *45*, 163–171. [CrossRef]
44. Oh, H.; Beum, H.T.; Lee, S.-Y.; Kim, J.; Kim, J.; Yun, Y.; Han, S.S. Bed configurations in CO vacuum pressure swing adsorption process for basic oxygen furnace gas utilization: Experiment, simulation, and techno-economic analysis. *Chem. Eng. J.* **2023**, *454*, 140432. [CrossRef]
45. Bashir, F.I.; Porter, R.T.J.; Catalanotti, E.; Mahgerefteh, H. Performance and cost analysis of pressure swing adsorption for recovery of H_2, CO, and CO_2 from steelworks off-gases. *Energies* **2025**, *18*, 2440. [CrossRef]
46. Javan-Bari, H.; Rafiee, R.; Bahadori, F. Simulation and multi-objective optimization of liquid hydrocarbons production by coupling blast furnace gas with coke oven gas of steelwork. *Clean Technol. Environ. Policy* **2023**, *25*, 2777–2788. [CrossRef]

47. Ling, Q.; Li, X.; Pei, Q.; Lei, Z.; Cui, P.; Xie, R.L. Analyzing the methanation thermodynamic feasibility of steel plant byproduct gases. *Sci. Rep.* **2024**, *14*, 12282. [CrossRef] [PubMed]
48. Zecca, N.; Boada, S.Z.; Spallina, V.; Manzolini, G. Integration of CASOH and DISPLACE technologies in a steel plant for the mitigation of CO_2 emissions—A techno-economic analysis. *Int. J. Greenh. Gas Control* **2025**, *147*, 104478. [CrossRef]
49. Xie, Y.; Xia, Z.; Li, C.; Mou, M.; Hu, X.; Chen, W.; Xu, X.; Xia, Y.; Liu, Z.; Fang, M. Pilot test and process modification of CO_2 chemical absorption for top gas recycling-oxygen blast furnace. *Sep. Purif. Technol.* **2025**, *370*, 133148. [CrossRef]

Disclaimer/Publisher's Note: The statements, opinions and data contained in all publications are solely those of the individual author(s) and contributor(s) and not of MDPI and/or the editor(s). MDPI and/or the editor(s) disclaim responsibility for any injury to people or property resulting from any ideas, methods, instructions or products referred to in the content.